Chapter 2

Three-dimensional bioprinting of skeletal muscle like tissue models

2.1. Introduction

Skeletal muscle tissue is one of the most widespread and dominant tissue types found in the human body, aggregating to nearly 45% of the body mass (Cittadella Vigodarzere and Mantero 2014; Ostrovidov et al. 2014). To maintain their primary activity of contraction and relaxation, these tissues require a steady supply of nutrients and metabolites that are generally provided by the networks of the vasculature (Cittadella Vigodarzere and Mantero 2014; Dennis and Kosnik 2000; G. Liu, Gabhann, and Popel 2012). Skeletal muscle tissue engineering (SMTE) aims to generate in vitro experimental models that can recreate the cellular niche of in vivo skeletal muscle tissue. Valid and functional models are constructed to explore the possible therapeutic opportunities for muscle tissue damage (Cittadella Vigodarzere and Mantero 2014; Ostrovidov et al. 2014). Damages and defects in the skeletal muscle tissue demand for the replacement of damaged tissue with a healthy one. Extensive lesions that impair the functions of muscle are commonly designated as volumetric muscle losses (VMLs) (Grogan, Hsu, and Skeletal Trauma Research Consortium 2011; Corona et al. 2015; J. T. Kim et al. 2016). Free standing flaps are used as the gold standard for the treatment of these lesions. The prime cause of the lesions being traumatic injuries and surgical resection of tumors that generally leads to donor site morbidity and has limited successful outcomes (Grogan, Hsu, and Skeletal Trauma Research Consortium 2011; Agostini, Lazzeri, and Spinelli 2013). The use of flaps, rather than grafts, is a necessity because grafts do not bring in their blood supply unlike muscle flaps that possess dense capillary network furnishing augmented blood flow into a hostile wound environment (Griffith et al. 2005; H. Bae et al. 2012; Shandalov et al. 2014; Villa et al. 2016; Klebuc and Menn 2013). SMTE provides therapeutic avenues for the restoration of volumetric muscle loss and medical interventions associated with skeletal muscle tissue (Syverud, VanDusen, and Larkin 2016).

Muscle tissue is universally known for its regenerative capacity (Perniconi and Coletti 2014). Nevertheless, upsetting cellular milieu resulting due to devastating situations like atrophy, wound, or diseases, may render the muscle tissue inoperative. Hence, the medical fraternity has been in dire need of an alternative model that replicates the in vivo like healthy and normal functioning of the muscle tissue. With the advent of the investigation carried out by Vanderburgh et. al. that used a simple method for three-dimensional (3D) culture of avian skeletal myotubes embedded in collagen gel, it was revealed that the introduction of the collagen gel could manifest the regulation of myotube differentiation (H. H. Vandenburgh, Karlisch, and Farr 1988). Dennis and Kosnik engineered three-dimensional skeletal muscle tissue constructs and termed them as "myooids" for the reason that they could mimic the inherent functional characteristics such as excitability and contractility of natural muscle tissue (Dennis and Kosnik 2000). The highlights of this work include self-produced extracellular matrix (ECM) by the myogenic cells that was used as a natural scaffold and self-contraction or self-structuring of the cell monolayer into a 3D structure between laminin-coated suture anchors in a 35 mm diameter culture dish. Potential techniques exploited in the fabrication of in vitro models of skeletal muscle tissues are micropatterning (Riboldi et al. 2008; Hosseini et al. 2012), micro-topography by chemical functionalization (Ker et al. 2011), mechanical conditioning by subjecting the cells to uniaxial and biaxial tensile strain to inculcate in them the ability to align and differentiate in vitro (Pennisi et al. 2011).

The techniques employed so far as indicated above clearly show that bi-dimensional cultures possess a limited capability in achieving the hierarchical organization of the muscle tissue with proper vascularization (Cittadella Vigodarzere and Mantero 2014). Therefore, such prevailing models of skeletal muscle tissue fabricated in an in vitro environment are unable to mimic the physiological microarchitecture of the inhabitant

muscles, refraining them from their characteristic structural and functional properties (Madden et al. 2015). The stymie presented above was overcome with the emergence of fused-deposition modeling (FDM) that lead to a novel approach for scaffold fabrication. This approach was further extended for printing cells-laden constructs, and the method is well-known as mechanical extrusion based 3D bioprinting (Ibrahim T. Ozbolat and Hospodiuk 2016a). 3D bioprinting is a representative of the melt-dissolution deposition technique (Chua and Yeong 2014; Bartolo 2011) in which a 3D structure is formed by the successive construction of one layer atop another. It aims at constructing a three-dimensional tissue by the repeated layering of thin films of cells (Atala 2004; Murphy and Atala 2014; I. T. Ozbolat and Yu 2013). Bioink is the printing material used for bioprinting and is customarily blended with cells to fabricate a cell-laden construct. To protect the cells from stresses appeared during the printing process, cells are often suspended in a growth medium or encapsulated in a hydrogel that provides them a supportive framework in their vicinity (Panwar and Tan 2016; Binder et al. 2011).

Unlike non-biological printing, 3D bioprinting involves additional complexities such as the choice of biocompatible materials, desired cell types, necessary growth and differentiation factors, and technical challenges related to the sensitivities of living cells and the construction of tissues (Yeatts and Fisher 2010). Bioprinting, however, has superior features compared to other biofabrication techniques. It enables fabrication of porous, anatomically correct, and precisely patterned cell-laden structures. This technique allows for controlled delivery of growth factors and genes. Also, the co-culture of multiple cell types and integration of vasculature provides an edge to this technology (Mehrban, Teoh, and Birchall 2016; Dababneh and Ozbolat 2014). Improvements and advances in the field of SMTE have elucidated that in order to maximize the therapeutic effects of cells and growth factors; clinically appropriate biomaterials are required as they

serve not only as templates for guiding tissue reorganization but also as matrices for providing optimum micro-environmental conditions to cells, as delivery vehicles for carrying bioactive factors to be released in a controlled manner, and as local niches to orchestrate in situ tissue regeneration (Koning et al. 2009; Bian and Bursac 2009; Langer and Vacanti 1993).

This chapter presents the fabrication of skeletal muscle tissue like models using a customized three-dimensional bioprinting system in combination with a novel bioink blend comprising of gelatin, sodium alginate and hydrolysed type-I collagen. The outcomes reveal that the bioprinter with customized specifications is capable of printing mouse myoblast (C2C12) cells-laden constructs with post-printing cellular viability of 80±5.73%. To achieve the appropriate state of bioink and its printability, various types of analytical examinations were performed, including the rheological characterization, swelling studies and the degree of porosity using scanning electron microscopy (SEM). Finally, bioprinted tissues were analyzed through the fluorescence imaging of live and dead cells as well as through visualization of actin filaments and nuclei together. The engineered skeletal muscle like tissues possess tremendous potential as an alternative model for in vitro physiological and toxicological-level studies, drug response studies, and therapeutic purposes, to name a few.

2.2. Materials and method

2.2.1. Materials

Dulbecco's Modified Eagle Medium (DMEM) [Himedia, Mumbai, India], Fetal Bovine Serum (FBS) [Himedia, Mumbai, India, Penicillin-streptomycin [Himedia, Mumbai, India,] Trypsin-EDTA [Himedia, Mumbai, India] and Phosphate buffer saline (PBS) [Himedia, Mumbai, India], Gelatin [Himedia, Mumbai, India], Collagen Type-I [Himedia, Mumbai, India], Sodium alginate pure [SRL, Mumbai, India], $CaCl_2$ [SRL,

Mumbai, India], Calcein AM [AAT Bioquest, Sunnyvale, California, USA], Ethidium homodimer III [AAT Bioquest, Sunnyvale, California, USA], Phalloidin Tetramethylrhodamine Conjugate [AAT Bioquest, Sunnyvale, California, USA], 4',6-diamidino-2-phenylindole (DAPI) [Himedia, Mumbai, India], Bovine serum albumin [Himedia, Mumbai, India], Paraformaldehyde [Himedia, Mumbai, India] and Triton x-100 [Himedia, Mumbai, India].

2.2.2. Culture of C2C12 myoblast cells

C2C12 mouse myoblast cells were procured from National Centre for Cell Science (NCCS) Laboratory, Pune. The cells were cultured on polystyrene culture plates and supplied with a culture medium containing 89% DMEM, 10% FBS, and 1% penicillin-streptomycin (100 µg/mL penicillin, 100 µg/mL streptomycin). The cells were grown at 37˚C in a standard CO_2 incubator [Eppendorf New Brunswick Galaxy 170S].

2.2.3. Preparation of bioink gel

Gelatin (Type B) was dissolved in PBS (pH=7.4) at a concentration of 15% (w/v). Sodium alginate powder was further added to the gelatin solution at the varying concentrations i.e., 1.5%, 2%, 3%, 5% and 7.5% (w/v) to form different gel compositions and they were further represented in the form of alginate:gelatin ratios 1:10, 1:7.5, 1:5, 1:3, 1:2, respectively. The prepared mixtures were stirred to dissolve thoroughly by heating on a magnetic hot plate stirrer set at 70˚C and 100 rpm for 60 minutes. The gels were allowed to cool in a sterile environment inside a biosafety cabinet. After the gel had cooled down to room temperature, hydrolyzed collagen type-I dissolved in PBS was added to the gel solution in order to achieve the final concentration of collagen about 0.5 % (w/v) within the hydrogel.

2.2.4. Development of the 3D bioprinting setup

A single nozzle 3D bioprinter was assembled and customized for the fabrication of all 3D constructs (cell-laden and without cells). The FDM (Fused Deposition Modelling) based 3D printer [Mendel Tricolor 3D printer, RepRap] for thermoplastics printing was assembled having NEMA-14 stepper-motors for driving the XYZ axes. The thermoplastics 3D printer was used for fabrication of a single nozzle hydrogel extrusion device [Paste Extruder, RichRap, open source] that can house one injection syringe (5 mL – 20 mL capacity) and can be driven by a belt-based pulley system using a single NEMA-14 stepper motor. The new single nozzle extruder was used to modify the thermoplastics 3D printer for cold extrusion of hydrogels using syringes and needles of various sizes. The needle size used for bio-printing was 21 gauge (0.514 mm inner diameter), and the total height of the construct for printing was kept at 350 microns. A sterile biosafety cabinet was used to house the custom-designed 3D bioprinter, and the environmental temperature of the printer was maintained between 25 °C - 30 °C for all the printing processes.

2.2.5. Bioprinting process

The hydrogel was loaded into a 10 mL syringe that was placed in the extruder mounted on the x-carriage. Using the custom-designed 3D bioprinter, constructs were fabricated in a layer-by-layer fashion with a cuboidal design of 25 x 25 mm cross-section and 1.2 mm (3 layers) thickness. The printing speed was kept at 15 mm/s, the grid infill density was set at 65%, and the extrusion multiplier kept between 0.05 - 0.2. The printing process was done at an environmental temperature ranging between 25 °C - 30 °C. The constructs, post-printing, were treated with 3% (w/v) $CaCl_2$ solution prepared in distilled water for 3-5 minutes to allow chemical cross-linking of the sodium alginate. The cross-linked

tissue constructs were gently washed 2-3 times using PBS and after that incubated in a culture medium at 37˚C with a 5% CO_2 supply.

2.2.6. Porosity measurement of the bioprinted constructs

The bioink blends consisting of varying concentration of alginate to gelatin (1:10, 1:7.5, 1:5, 1:3, 1:2) were used for fabrication of constructs. Scaffolds of various bioink compositions ranging the volumetric size of 15 x 15 x 1.4 mm^3 with 65% filling density were printed and cured. Constructs having different alginate-gelatin ratios were incubated in 35-mm Petri dishes immersed in 2 mL of PBS. After the swelling equilibrium was reached, PBS was drained completely, and the constructs were then lyophilized. The lyophilized samples were further coated with gold for SEM imaging using a Zeiss EVO 18 SEM [Zeiss, Oberkochen, Germany] at 20 kV. The pores were measured using ImageJ software (NIH, USA) from at least five different images of each type of construct. The pore size distibution of the various constructs was plotted using Origin software [OriginLab Corporation].

2.2.7. Swelling study

Constructs having different alginate-gelatin ratios were weighed, and their initial weight was recorded before and after treatment with $CaCl_2$. The constructs were then incubated in 35-mm Petri dishes immersed in 2 mL of PBS. The PBS was drained completely, and the constructs were again weighed after 3, 6, 9, 15 and 27 h. The printed constructs were observed until saturation of weights. The swelling data was plotted using Origin [OriginLab Corporation].

2.2.8. Rheological properties of the bioink

The rheological properties of the chosen bioink composition i.e.; alginate:gelatin ratio of 1:5 (3% (w/v) sodium alginate, 15% (w/v) gelatin and 0.5% (w/v) hydrolysed collagen type-I composition were analyzed with a viscometer [Brookfield LV DV-II+ Pro, CPE-

42 Probe]. Solutions were kept at varying temperatures before data acquisition. The test was performed in an environment consistent with the temperature of bioprinting. Bioink gel samples were tested at speed ranging from 1/min to 5/min as well as at temperatures ranging from 27.5 °C to 45 ˚C.

2.2.9. Cell encapsulation and bioprinting

C2C12 mouse myoblast cells were dissociated from culture dishes using trypsin-EDTA [0.25%, HiMedia] solution. The cells were re-suspended in cell culture media for counting. After counting, the cell suspension was gently mixed with the optimized composition of hydrogel to achieve a final concentration of 10^7 cells/mL of bioink. The hydrogel bioink was loaded into a 10 mL syringe that was placed in the extruder mounted on the x-carriage. Using the custom-designed 3D bioprinter, constructs were fabricated in a layer-by-layer fashion with a cuboidal design of 25 x 25 mm cross-section and 1.2 mm (3 layers) thickness. The printing speed was kept at 15 mm/s, the grid infill density was set at 65%, and the extrusion multiplier kept between 0.05 - 2.0. The printing process was done at an environmental temperature ranging between 25 °C - 30 °C. The constructs, post-printing, were treated with 3% (w/v) $CaCl_2$ solution prepared in distilled water for 3-5 minutes to allow chemical cross-linking of the sodium alginate. The cross-linked tissue constructs were gently washed 2-3 times using PBS and after that incubated in a culture medium at 37˚C with a 5% CO_2.

2.2.10. Cell viability analysis in bioprinted constructs by live/dead assay

Cell survival in the 3D printed cell-laden constructs was examined at different time points after fabrication of the tissue constructs to determine the influence of the printing process on cell viability as well as to assess the potential of long-term cell viability within the constructs. Fluorescence-based live/dead assay was carried out according to the manufacturer's instructions. The constructs were stained with a solution containing 2 μM

Calcein AM and 4μM Ethidium homodimer III for 60 minutes in the dark at 37°C. A Nikon Ti-U [Nikon, Japan] fluorescent microscope was used for image acquisition. The tissue constructs were stained after 3 h, 1 day, 7 days and 14 days after fabrication. At least five images were captured across various focal planes and locations were used to count the live and dead cells using ImageJ software. The cell viability was then calculated as the percentage of the number of live cells to the total number of cells.

2.2.11. Visualization of actin filaments and nuclei

For observation of the actin filaments (F-actin) and nuclei of the cells encapsulated within the printed 3D tissue constructs, fluorescence staining of F-actin and nuclei was performed for the printed constructs at different time points following incubation. The samples were fixed with 4% (w/v) paraformaldehyde for 15 min and then immersed in 0.1% (v/v) Triton X- 100 in PBS for 30 min for permeabilization of the cell membrane. It was followed by blocking with 1% (w/v) bovine serum albumin (BSA) in PBS for 1 h at room temperature. For F-actin cytoskeleton staining, the samples were then soaked in 1:1000 dilution of Tetramethyl-rhodamine-phalloidin in 0.1% (w/v) BSA for 1 h at 37°C. The nuclei were further stained with 4, 6-diamidino-2-phenylindole (DAPI) (1μg/mL) for 30 min at 37°C. The samples were then examined using a Nikon TiU inverted fluorescence microscope.

2.2.12. Image and statistical analysis

The fluorescent images were processed using ImageJ software in order to remove the background noise. The fluorescent images were separately convolved with Gaussian blur function and subtracted from their respective original images to remove the background noise. For counting of the live and dead cells, the processed images were first converted to grayscale images followed by thresholding and watershed. Thereafter, the particle analyzer tool was used for automated counting of the number of viable and dead cells

within the images. Statistical analysis was performed using Origin. The data were collected from at least 3-5 parallel samples. Statistical analysis was performed by using one way ANOVA post hoc Tukey means of comparison. All the data are represented in the form of mean±standard deviation (SD).

2.3. Results and discussion

2.3.1. Bioprinting setup and bioink properties

The schematic diagram in Figure 2.1 shows the structural components of the bioprinting system and the working setup that is used for creating multi-layered microporous scaffolds and tissue constructs. The device is equipped with a micro-extrusion assembly that includes a manually assembled single nozzle bioprinting head integrated with a custom-made pulley based drive that enables continuous dispensing of both cells-free and cells-laden bioink blends. The modified 3D bioprinter is upgradable to 3 nozzle hydrogel extrusion device using an open source X-carriage extension and the control board of the reminiscent tricolor 3D printer. Such an approach of using a desktop 3D printer for modification not only allows for a customizable, inexpensive and easy to use system capable of fabricating tissue analogs, it also empowers research labs which cannot afford to have highly expensive medical grade high-end 3D bioprinters (Goldstein et al. 2016). The bioink blend is composed of gelatin, sodium alginate and hydrolyzed collagen type-I. The bioink components have been successfully applied for bioprinting in the recreation of various in vitro tissue models (B. Duan et al. 2013; Zhao et al. 2014). Biomaterials used in the fabrication of bioprinted tissue constructs are being chosen based on ease of availability, low cost and their usage require minimal technical expertise. Alginate an anionic polysacchride is a promising biomaterial as it easily forms hydrogels by $Ca^{2+/}Na^{+}$ ion exchange. It is widely used for bioprinting due to its shear thinning behaviour. However, it is also associated with a lack of cell binding domains. Blending of gelatin

with alginate improves the cell supportive environment of the alginate (B. Duan et al. 2013).

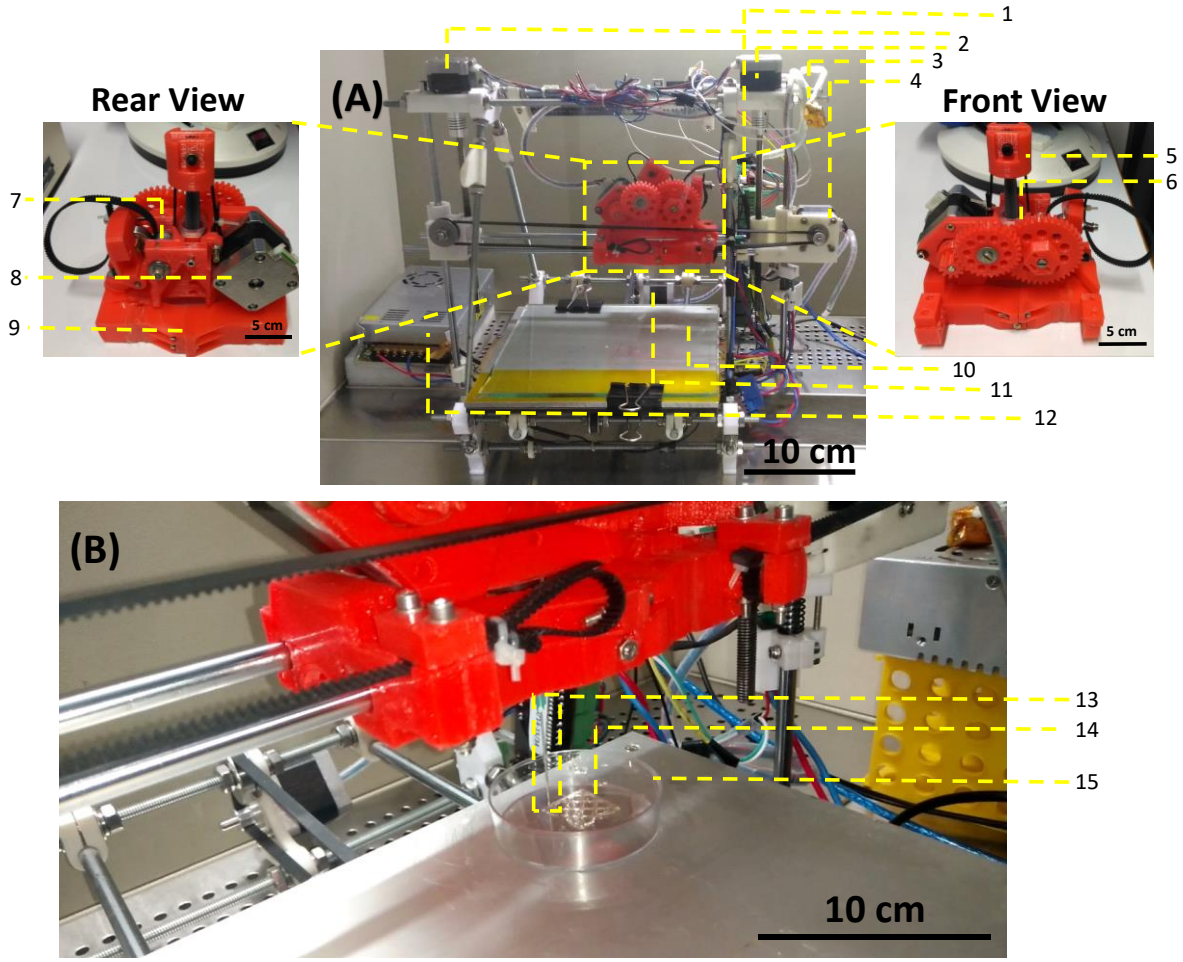

Figure 2.1 Representative images show (A) The structural components of a custom-designed bioprinting system and (B) Bioprinting of a multi-layered tissue construct in Petri dish using the same setup. Labelled numbers indicate: 1- PCB control board, 2- Z-axis stepper motor, 3- Extruder temperature sensor, 4- X-axis stepper motor, 5- Syringe plunger cap, 6- Syringe holder, 7- Belt and pulley-based extrusion drive, 8- Stepper motor for extrusion, 9- Modified X-axis carriage, 10- Printing bed, 11- Y-Axis stepper motor, 12- Power supply, 13- Syringe needle extruding the material, 14- Printed construct and 15- Petri plate.

3D bioprinting of such blends allows the fabrication of constructs but, has problems with spreading of the cells (Zhao et al. 2014). So, in order to further support the cells the alginate gelatin blend is added with collagen type I. Both the gelatin and the hydrolysed type-I collagen are known to provide adhesive moieties for the cells within the scaffolds (Grzesik and Robey 1994;Ibrahim T. Ozbolat and Hospodiuk 2016; Panwar and Tan

2016). Bioink formulation with fibrillated collagen type-I as main component for extrusion bioprinting has problems with respect to its viscosity and inability to be rapidly crosslink (Wu et al. 2016). So, alternatively hydrolysed collagen type-I can be used for the purpose. Hydrolysed collagen type-I are small molecular weight (6-10 kDa) polypeptides which are synthesized by enzymatic hydrolysis of denatured collagen or gelatin. These polypeptides show better solubility, absorbency and biodegradability compared to its sources (Ficai et al. 2013; Pei et al. 2013). It also shows excellent biocompatibility as it supports cell adhesion and proliferation (Kim, Kim, and Salih 2005; Ramadass et al. 2014).

The mechanism of scaffold fabrication is based on the two independent processes that take place within the bioink blend during bioprinting. While printing, the thermo-reversible nature of gelatin helps to stabilize and temporarily provide structural stability to the bioink at a temperature ranging between 25°C - 30°C. Later, the crosslinking of sodium alginate with calcium (Ca^{2+}) ions was achieved by soaking of the constructs in calcium chloride ($CaCl_2$) solution that led to the stability of the constructs at an incubation temperature of 37°C. It was crucial for $CaCl_2$ to penetrate the bioprinted bioink mass to ensure the mechanical integrity and self-sustenance of the construct at later stages of incubation as well as to facilitate cellular growth within the constructs.

Although alginate is generally considered to provide the mechanical support to constructs, it acts as a barrier for cell spreading and cellular interaction within the constructs due to its slower rate of in vitro degradation. So, an inclusion of higher concentration of gelatin and collagen would favour optimal growth and differentiation of cells within the constructs. Therefore, keeping the concentrations of gelatin (15% (w/v)) and hydrolysed type-I collagen (0.5% (w/v) of bioink) constant, the appropriate concentration of alginate was optimised and chosen amongst its several concentrations tested (1.5%, 2%, 3%, 5%

and 7.5% (w/v)). For this purpose, swelling behaviour and porosity measurement of the above mentioned compositions was used as a criteria to select the bioink blend for cell applications.

2.3.2. Bioprinting of porous scaffold and their characterization

Porosity of biomaterial scaffold is of great significance as it provides tissue forming microenvironment which facilitates cell proliferation, migration and ECM production (Loh and Choong 2013). Ideally tissue engineering scaffolds are desired to provide variation in pore size at different stages of tissue formation. During the initial stage a low porosity is preferred in order to provide structure fidelity and protection to the associated cells. At later stages of tissue development, the scaffolds need to progressively provide greater pore size to facilitate tissue formation (Han et al. 2013). Figure 2.2 represents the scanning electron micrographs of varying compositions of printed constructs. The dimensions of the pores present within the constructs were measured. The results of the analysis are as shown in Figure 2.3. The figure shows a plot of percentage of pores vs pore size. The results indicate an increase in the size of pores with the decrease in the alginate concentration of the bioink blend. The shape of pores within the constructs printed using the bioink blends ranged from spherical to ellipsoidal as evident from the SEM images in figure 2.2.

Swelling behaviour of hydrogel material is an important physiochemical parameter as it gives a general idea of the capacity of the biomaterial to imbibe water due to the presence of hydrophilic functional groups which are attached to polymeric backbone. On the other hand, presence of crosslinked polymeric backbone prevents the hydrogel from getting totally dissolved (Gerlach and Arndt 2010). In a similar manner the swelling characteristic of the bioink after printing is important to understand if the bioink would be suitable for transport of nutrients, gases and waste products. Additionally, it also gives an idea of the

whether the crosslinking of bioink was enough for the structure fidelity of the bioprinted constructs (Shim et al. 2011). Scaffolds of various bioink compositions with dimensions of 25 x 25 x 1.2 mm^3 with 95% filling density were printed and cured. The swelling study conducted on the different printed constructs shows the uptake of PBS and swelling of the constructs by nearly 30% in weight from their initial weight within 27 h of incubation (Figure 2.4). Given the outcomes obtained from analysis of SEM images and the swelling study, the composition of the bioink blend 1:5 exhibited a high precentage of smaller dimension pores comparable to the size of C2C12 cells with good swelling behaviour hence the composition would provide encapsulation for larger number of cells with good shape fidelity. Consequently, the alginate:gelatin ratio of 1:5 was chosen for further evaluation of compatibility for bioprinting and embedding of C2C12 cells.

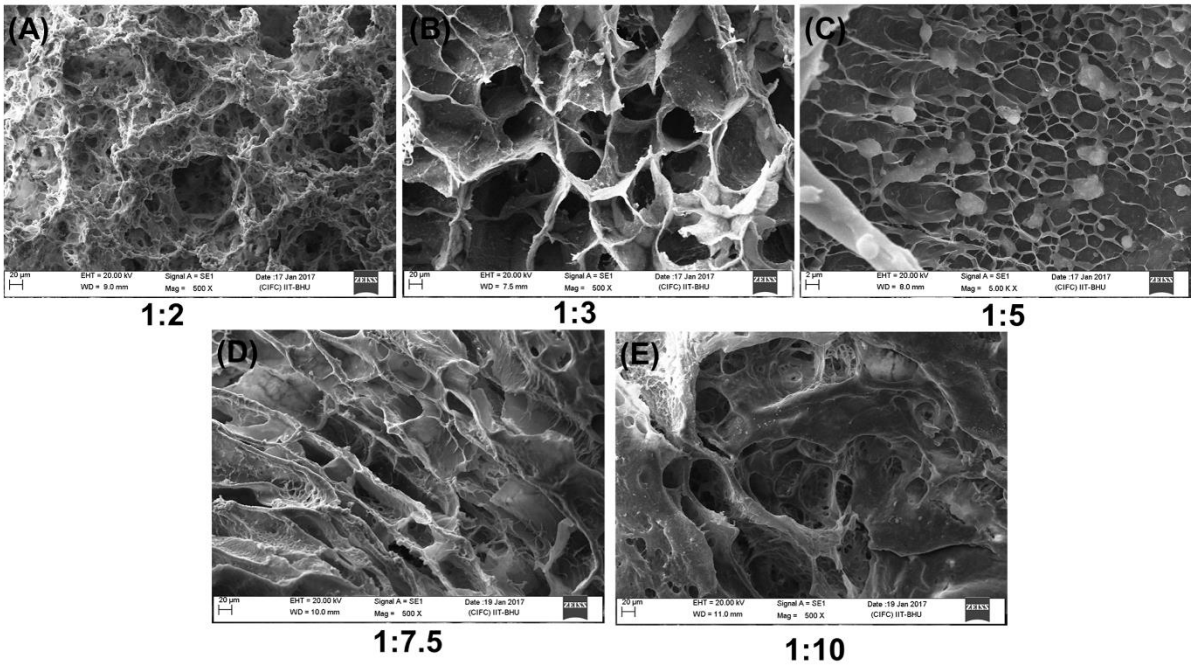

Figure 2.2 SEM photomicrographs showing the pores present within the various alginate: gelatin bioink compositions.

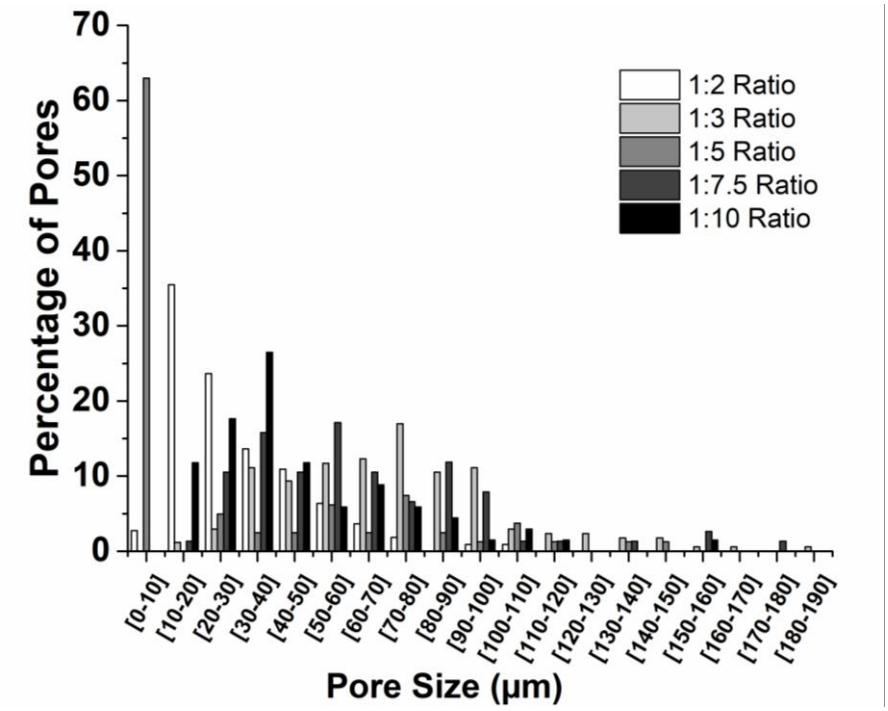

Figure 2.3 Pore size distribution analysis results of printed constructs using alginate: gelatin bioink compositions.

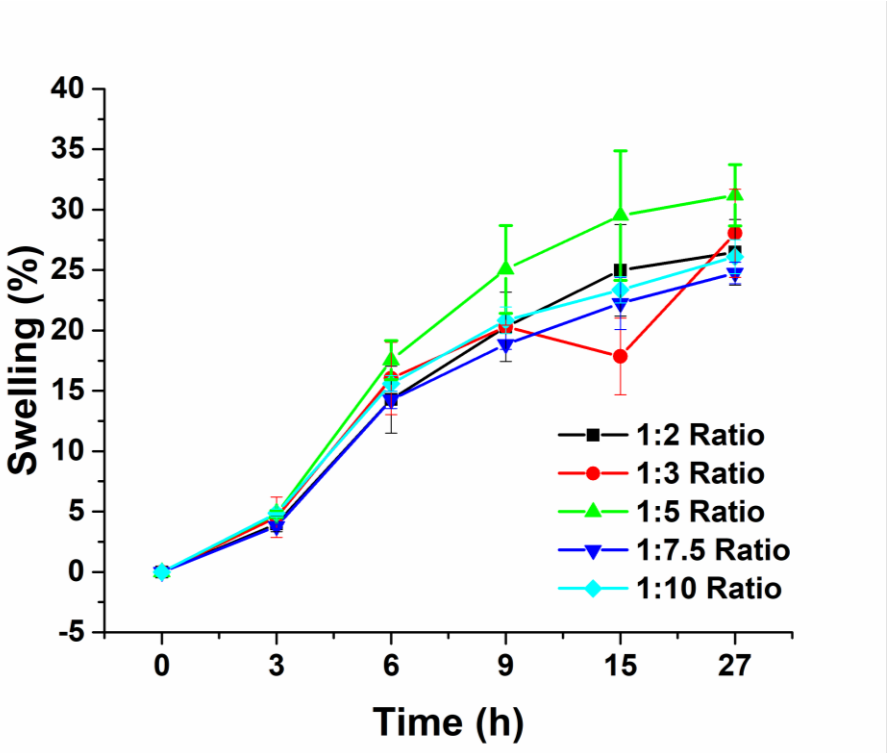

Figure 2.4 Swelling studies results of the 3D printed constructs using various alginate: gelatin bioink compositions.

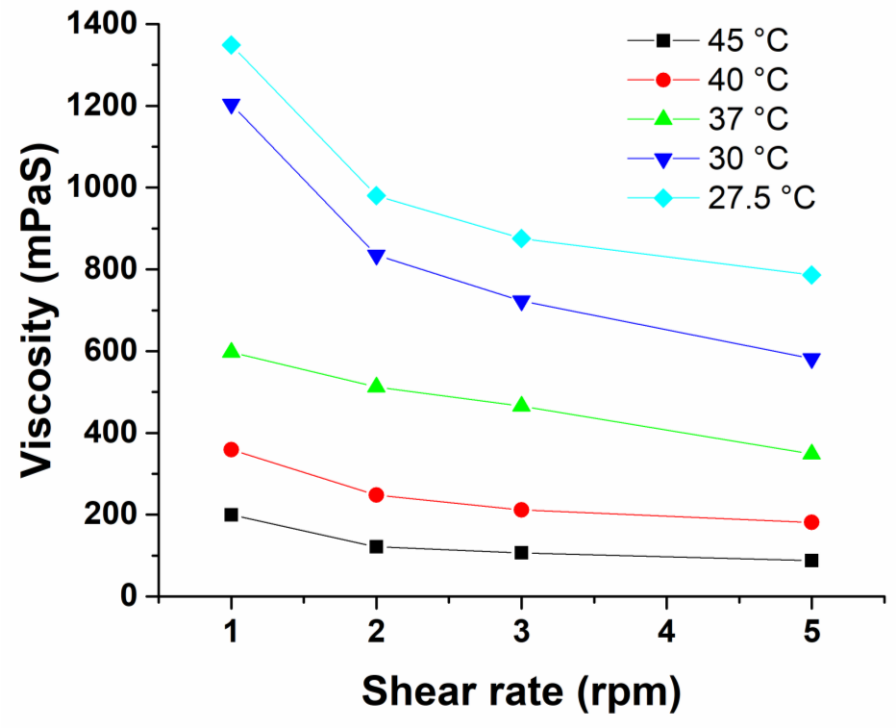

Figure 2.5 Rheological study results showing the variation in viscosity with respect to shear rate for the chosen 1:5 composition bioink at various temperatures.

The chosen bioink blend i.e., alginate:gelatin ratio of 1:5 (3% (w/v) sodium alginate, 15% (w/v) gelatin and 0.5% (w/v) hydrolysed type-I collagen) was characterized by measuring its viscosity at varying temperatures (Figure 2.5). The results revealed that the viscosity of the bioink blend increases with decrease in temperature as well as applied shear force, thereby increasing the fidelity. The change in viscosity of the bioink can be observed to be less steep as temperature is increased from 30°C to 45°C. Such an observation is due to the thermoreversible behaviour of major bioink component gelatin. Gelatin behaves as a hydrogel like substance below its sol gel temperature of 30°C. Increase in temperature above the transition temperature leads to aqueous nature of gelatin and reduction in its viscosity, and hence a decrease in bioink viscosity with increase in temperature is observed (Zhang, Li, and Shi 2006). The results also revealed that the viscosity of the bioink blend increases with decrease in temperature as well as applied shear force, thereby increasing the fidelity. This may have various consequences on the fate of the cells; a

decreasing temperature for bioprinting may increase the viscosity of the gel, which along with the alginate content may hinder the spreading of the cells.

In Figure 2.5 it can be seen that at 27.5°C and 30°C, the viscosity of the bioink blend consisting of an alginate:gelatin ratio of 1:5 (Figure 2.5) decreased from 1349 mPas to 786.2 mPas and 1204 mPas to 449 mPas at shear rates ranging from 1/min to 5/min, respectively. The drop in the viscosity values at higher shear rates, at constant temperature is conclusive of the shear thinning behaviour of the bioink composition that helps in clogging free continuous micro-extrusion at various deposition rates. The shear thinning behaviour of the bioink blends is an essential property for bioink compositions, which enables printing of various shapes and sizes of scaffolds at varying resolutions of bioink extrusion.

2.3.3. Bioprinting of cells-laden in vitro tissue constructs

Ensuing with our selected bioink composition (i.e gelatin (15%), sodium alginate (3%), and hydrolysed collagen type-I (0.5%)) C2C12 were added at a density of 10^7cells/mL of bioink resulted in a decrease in viscosity of the bioink. This decrease in viscosity was compensated by lowering the temperature below 30°C and cells-laden skeletal muscle cell constructs were very easily bioprinted through our system.

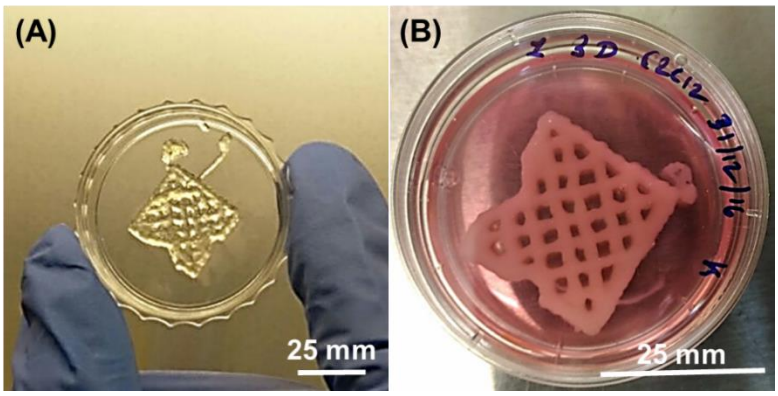

Figure 2.6 Images of bioprinted constructs with a cuboidal shape with dimensions of 25 x 25 x 1.2 mm^3 (A) Represents the image of a just bioprinted construct (B) Represents the image of C2C12 cell laden bioprinted construct in cell culture media.

Figure 2.6A, B shows the image of just bioprinted construct and bioprinted construct in culture repectively. A healthy population of C2C12 cells was cultured and harvested to achieve the appropriate cell density for encapsulating them into the bioink blend (Figure 2.7A). Cells were characterized by their viability status using live/dead assay (Figure 2.7A) and staining of actin filaments and nuclei (Figure 2.7B). Thereafter, the bioink blend with cell density at 10^7 cells/mL of bioink was bioprinted into constructs of cuboidal shape (25 x 25 x 1.2 mm^3) with 65% infill density (Figure 2.6A, B). The bioprinted constructs were achieved along with apt structural stability and integrity of the constructs for more than 14 days of culture. Bright field images of the bioprinted constructs also revealed that the myoblast cells were distributed in various layers of the constructs, and they were proliferating in numbers after the 5^{th} day of incubation (Figure 2.7C left). This indicates the suitability of the constructs for myoblast cells. Representative images display the 3D organization of myoblasts and their intercellular interaction within the constructs (Figure 2.7C right). The amount of pressure applied by the printing system was found to be non-detrimental for the viable cell population. The viability assay of embedded cells after 3 h, 1 day, 7 days and 14 days of culture (Figure 2.8A) revealed that the percentage of viable cells progressively rose with in vitro culture time over a period of 14 days. Also, quantitative analysis of live cells after 3 h, 1 day, 7 days and 14 days of incubation of the tissue constructs indicated that the cell population was stable ranging the viability above 90% for the extended periods (Figure 2.8(B)). Indeed, the printing process was found significantly consistent for achieving similar levels of the viability of cells embedded within the printed constructs (Figure 2.8(C)).

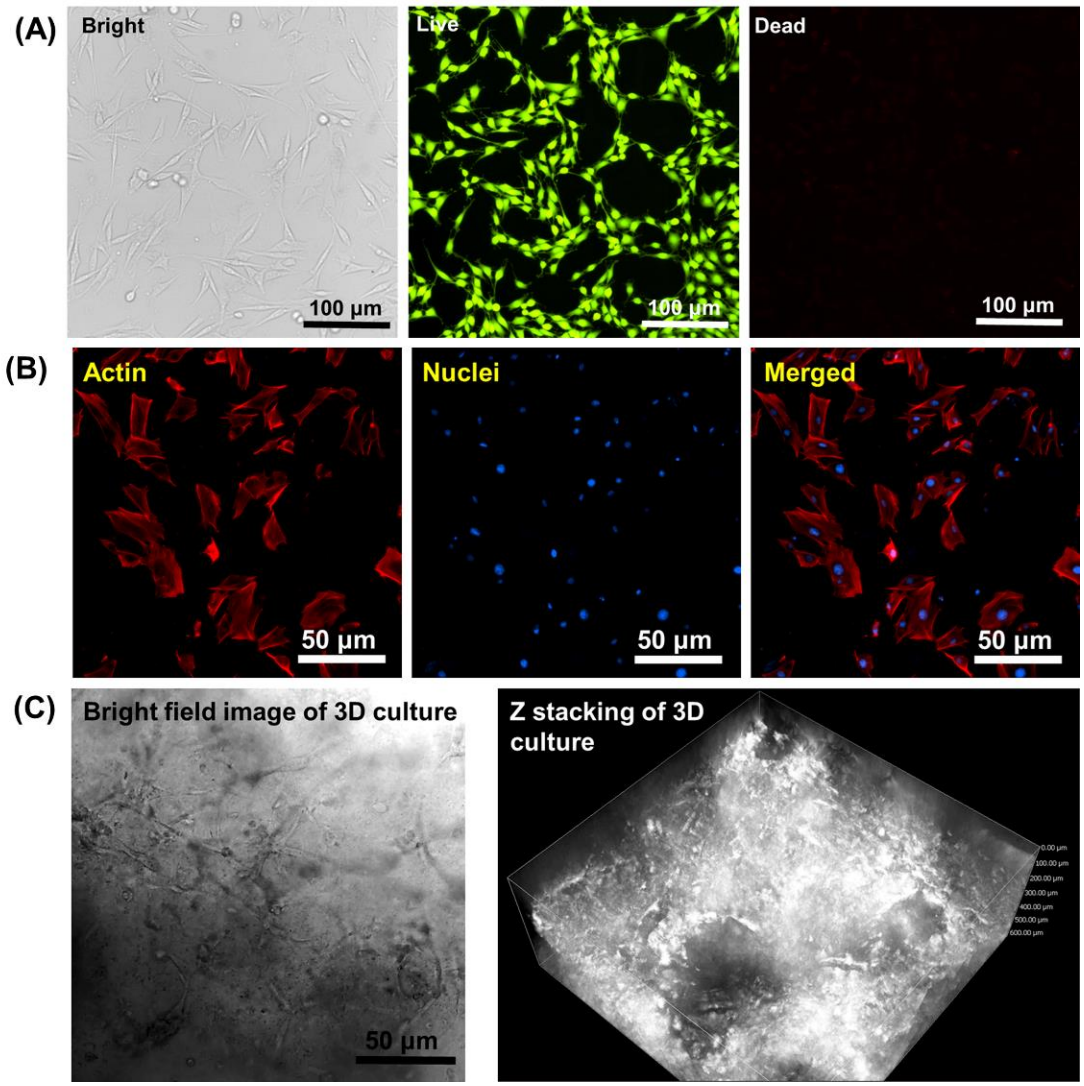

Figure 2.7 (A) Bright-field images of C2C12 mouse myoblast cells cultured on standard Petri dish, C2C12 stained by calcein-AM for assessing the live cells (green in color), and C2C12 stained by ethidium homodimer for assessing the dead cells (red in color) and nuclei with DAPI (blue in color) in C2C12 cells. (B) Represents the visualization of actin filaments stained with rhodamine phalloidin (red in color) and nuclei with DAPI (blue in color) in C2C12 cells. (C) Representative image on the right reveals the morphology of the cellular networks formed within the printed tissue constructs after 5^{th} day of culture. Image on the left is Z stacked image of printed tissue constructs after 5^{th} day of culture.

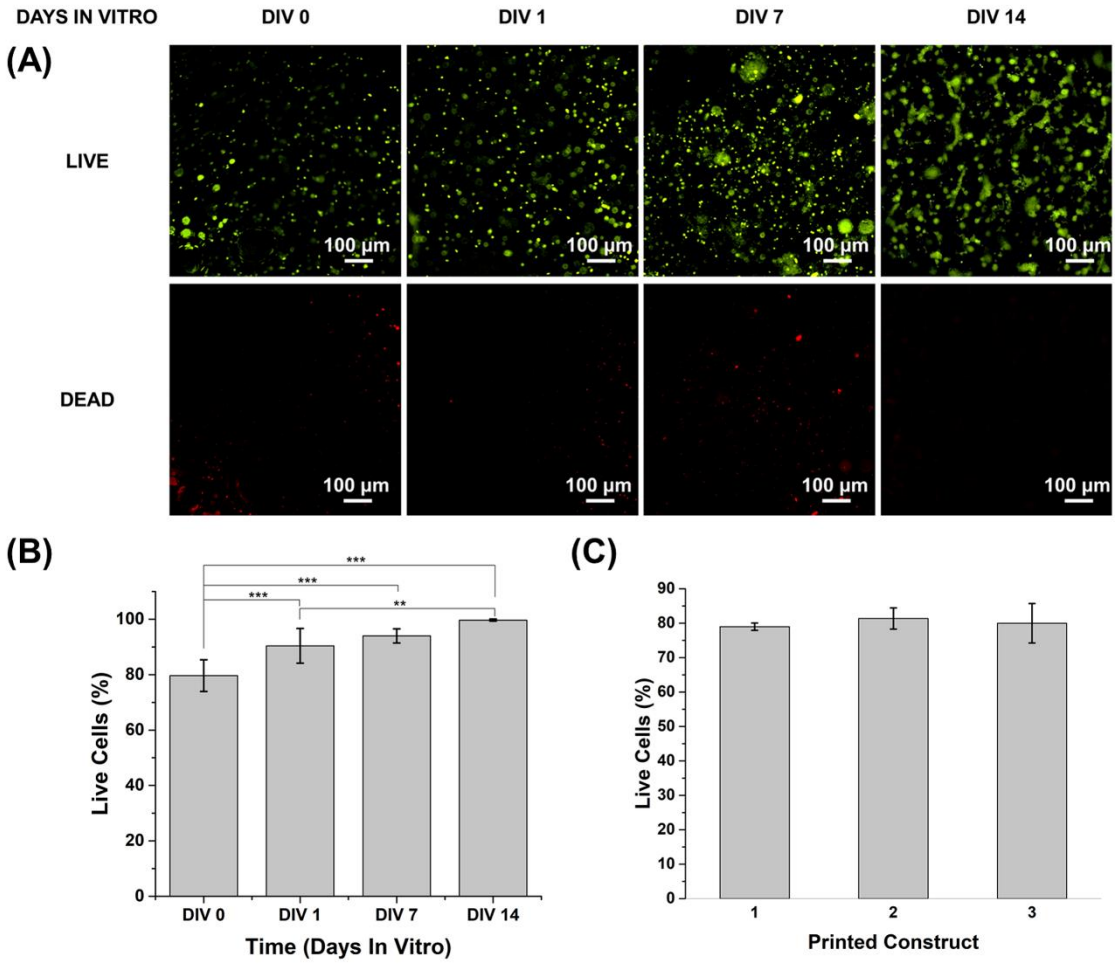

Figure 2.8 (A) Representative images show the live (green in color) and dead (red in color) cells (i.e., mouse myoblast C2C12 cells) of the printed tissue constructs at different time points. (B) Quantitative analysis of live cells after 3 h, 1st day, 7th day and 14th day of incubation of the printed tissue constructs.Significance levels are presented as ***p<0.001, **p<0.01. (C) The graph showing percentage of viable cells within the constructs after 3 hours of incubation printed at different instances. This shows the consistency of the printing process for achieving similar viability of cells within the printed constructs.

Also, the staining of nuclei and F-actin revealed that some of the C2C12 cells have started to physically communicate using the interconnective pores of the bioink after 14 days of culture (Figure 2.9). These constructs in culture demonstrate the potential efficacy of our bioink composition and the optimal nature of our bioprinting technique for fabrication of near physiological skeletal muscle in vitro tissue model.

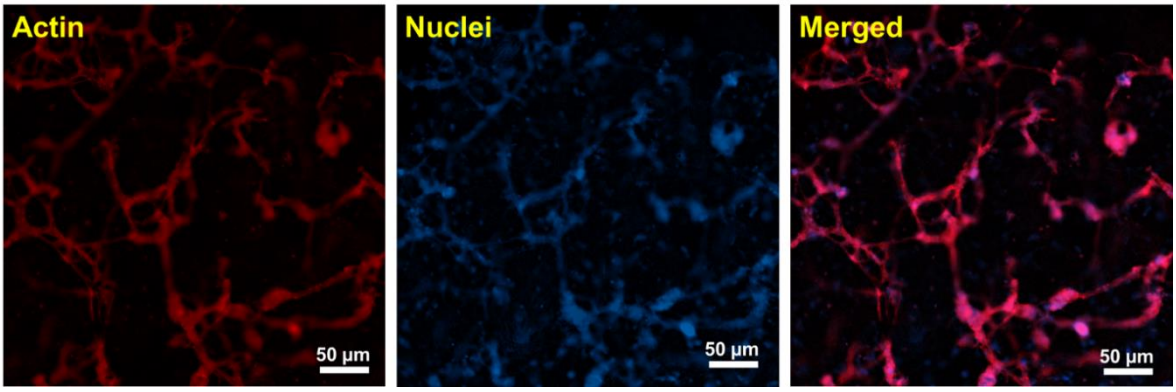

Figure 2.9 Fluorescent images showing the filamentous actin (red in color) and nuclei (blue in color) of cells embedded within the printed constructs after 14 days of incubation.

Similar to the study, various 3D bioprinting studies have been carried out using alginate, gelatin and collagen type-I as bioink components. Duan et. al reported the use of gelatin (0.06 g/mL) and alginate (0.05 g/mL) in sodium chloride solution for bioprinting aortic valve leaflet interstitial cells (VIC) and aortic root sinus smooth muscle cells (SMC) ($2x10^6$ cells/mL) in the form of hydrogel discs. Although they found the encapsulated cells to be viable for up to 7 days, the cell viability of 86.0 ± 4.6% and 84.6 ± 5.1% for VIC and SMC cells respectively after 7 days. Also, VIC and SMC cells maintained their spherical morphology after seven days of printing (B. Duan et al. 2013). Zhao et al. referred to a bioink which composed of 10% w/v gelatin, 1% w/v sodium alginate and 2% w/v fibrinogen seeded Hela cells ($1x10^6$ cells/mL). The alginate was chemically crosslinked using $CaCl_2$ (3% w/v) followed by crosslinking of fibrinogen using thrombin (20U/mL) for 15 minutes. They reported cell viability of 94.9% ± 2.2% after 8 days of printing. The Hela cells showed round spheroid morphology with cell to cell physical communication (Zhao et al. 2014). Another bioprinting study by Ouyang et al reported alginate 1% w/v, gelatin 10% w/v and fibrinogen 2% w/v and HEK 293FT based bioinks resulted in constructs with cells having similar round spheroid like cell morphology (Ouyang et al. 2015). With an intenstion of improving the biomimetic environment of the cells, Wu et al. printed a bioink consisting of human corneal epithelial cells (10^7

cells/mL), sodium alginate 1% w/v, gelatin 10% w/v and collagen type I (0.08 %) w/v. The human corneal epithelial cells in bioprinted constructs showed a post print viabilty of over 94% and also remained viable for a period of 8 days. The addition of fibrous collagen type-I increased the biomimetic porperty and cellular proliferation in the constructs but, the cells were still associated with round spheroid like morphology despite the application of sodium citrate for degradation of alginate (Wu et al. 2016). In contrast to these studies, the current study involved a bioink consisting of C2C12 cells (10^7 cells/mL), gelatin 15% w/v, alginate 3% w/v and 0.5% w/v hydrolysed collagen type I. Although, the bioprinted constructs showed a post print viability of around 80%, the cells have proliferated in the subsequent days reached above 90% at 7 day and retained the status till 14 days. Comparable results of cell viabilty were seen in previously disscussed studies. A common problem observed in the alginate-gelatin bioink systems was the formation round cell morphology this has been attributed to the presence of alginate. In the current study, the cells within the bioinks showed a well spread morphology after 14 days of in vitro culture. This observation may be due to the presence of higher concentration of cell adhesive moeities contributed by the addition of a higher concentration of 15% gelatin in comparison to 10% other studies. Intrestingly despite the addition of 3% sodium alginate the bioink has provided sufficient flexibility in order for the remodelling of the scaffold, spreading of cells and formation of intercellular networks. This may be due to additional source of cell adhesive groups given by hydrolysed type I collagen, which may also serve as source of small peptides necessary new ECM formation. Thus, a new bioink composition including gelatin 15%, alginate 3% and hydrolysed collagen 0.5% with C2C12 cells was bioprinted into constructs which showed viability for period of 14 days along with improved cell spreading behaviour.

2.4. Summary

To summarise, a customized microextrusion bioprinter was assembled and applied for printing three-dimensional mouse myoblast (C2C12) cells-laden model tissue constructs. The C2C12 cells show high cell viability (>80%) immediately post printing showing the efficacy of the printing process. The encapsulated cells manifest an increase in the viability percentage for the extended periods, observed at least for 14 days of incubation. In addition, the composition of the optimized bioink blend exhibits the necessary characteristics for bioprinting process as well as for the growth and physical communication of the encapsulated C2C12 cells, as can be seen from the representative images of cell morphology and the viability assay. In total, a simple and cost-effective strategy was developed by combining inexpensive bioprinting system and novel bioink composition for the potential development of skeletal muscle like tissue models.